

SAND-98-1044C
CONF-980708--**RESULTS OF STEEL CONTAINMENT VESSEL MODEL TEST¹**

Vincent K. Luk, John S. Ludwigsen, and Michael F. Hessheimer
Sandia National Laboratories, Albuquerque, NM, USA

Kuniaki Komine
Nuclear Power Engineering Corporation, Tokyo, Japan

Tomoyuki Matsumoto
Hitachi Ltd., Hitachi-shi, Ibaraki-ken, Japan

James F. Costello
United States Nuclear Regulatory Commission, Washington, DC, USA

RECEIVED
JUN 02 1998
QSTI

ABSTRACT

A series of static overpressurization tests of scale models of nuclear containment structures is being conducted by Sandia National Laboratories for the Nuclear Power Engineering Corporation of Japan and the US Nuclear Regulatory Commission. Two tests are being conducted: a test of a model of a steel containment vessel (SCV) and a test of a model of a prestressed concrete containment vessel (PCCV).

This paper summarizes the conduct of the high pressure pneumatic test of the SCV model and the results of that test. Results of this test are summarized and are compared with pretest predictions performed by the sponsoring organizations and others who participated in a blind pretest prediction effort. Questions raised by this comparison are identified and plans for posttest analysis are discussed.

INTRODUCTION

The Nuclear Power Engineering Corporation (NUPEC) of Japan and the US Nuclear Regulatory Commission (NRC) are co-sponsoring a Cooperative Containment Research Program at Sandia National Laboratories. The purpose of the program is to investigate the response of representative models of nuclear containment structures to pressure loading beyond the design basis accident and to compare analytical predictions with measured behavior. This is accomplished by conducting static, pneumatic overpressurization tests of scale models at ambient

temperature. This paper describes the conduct and results of the high pressure test of the SCV model.

MODEL DESCRIPTION

The SCV model is representative of the steel containment vessel of Improved Mark II Boiling Water Reactor plants in Japan. The geometric scale is 1:10. Since it was desired to use the same materials for the fabrication of the model as are used in the construction of the actual plants, the scale on the wall thickness was set at 1:4. The portion of the model above the material change interface which is slightly below the equipment hatch centerline (see Fig. 1) was fabricated of SGV480, a mild steel, while the lower portion of the model and the reinforcement plate around the penetration were fabricated from high strength SPV490 steel. The equipment hatch cover and top head were non-functional in the model and were welded shut. Whereas the design pressure of the prototype containment is 0.31 MPa (45 psig), the scaled design pressure, P_{ds} , for this mixed scale model is 0.78 MPa (113 psig).

The model was fabricated at the Hitachi Works in Japan and shipped to Sandia National Laboratories in the US for instrumentation and testing. After delivery to Sandia, a 38 mm thick steel (ASTM SA516 Grade 70) contact structure (CS) was installed over the SCV model prior to testing to represent some features of the reactor shield building in the actual plant. A nominal gap of 18 mm was maintained between the SCV model

¹ This work is jointly sponsored by the Nuclear Power Engineering Corporation and the US Nuclear Regulatory Commission. The work of the Nuclear Power Engineering Corporation is performed under the auspices of the Ministry of International Trade and Industry, Japan. Sandia National Laboratories is operated for the US Department of Energy under Contract Number DE-AC04-94AL85000.

MASTER**DTIC QUALITY INSPECTED 1***ph*

DISCLAIMER

This report was prepared as an account of work sponsored by an agency of the United States Government. Neither the United States Government nor any agency thereof, nor any of their employees, makes any warranty, express or implied, or assumes any legal liability or responsibility for the accuracy, completeness, or usefulness of any information, apparatus, product, or process disclosed, or represents that its use would not infringe privately owned rights. Reference herein to any specific commercial product, process, or service by trade name, trademark, manufacturer, or otherwise does not necessarily constitute or imply its endorsement, recommendation, or favoring by the United States Government or any agency thereof. The views and opinions of authors expressed herein do not necessarily state or reflect those of the United States Government or any agency thereof.

and the CS. A schematic of the SCV/CS assembly is shown in Fig. 1. Instrumentation of the model consisted of over 800 channels of data, including strain gages, displacement transducers, temperature and pressure sensors, acoustic emission device as well as video monitoring.

TEST OBJECTIVES

The objectives of the SCV model test were:

1. to provide experimental data for checking the capabilities of analytical methods to simulate the pressure response of a steel containment vessel into the inelastic range and after making contact with the CS,
2. to investigate the failure mode(s) of the SCV model, and
3. to provide experimental data useful for the evaluation of actual steel containments.

PRETEST ANALYSIS

Pretest finite element analyses were performed to predict the behavior of the model, guide the placement of instrumentation, and identify and evaluate failure modes. Details of the analysis are provided (Porter et al., 1996). In addition to predicting the global response of the model, these analyses, based on the design configuration, predicted high strains in the shell surrounding the equipment hatch reinforcement plate, with the highest strains in the lower strength SGV480 shell. Generalized contact between the SCV model and the CS was predicted to occur around 4.2 MPa (600 psig) and the most likely failure mode predicted was a local ductile failure at a locally thinned area in the SPV 490 shell adjacent to the equipment hatch at a pressure of 4.5 MPa (650 psig). These predictions were qualified by uncertainties about the as-built configuration of the model.

In addition to the pretest analysis performed by Sandia, several organizations participated in a blind, pretest prediction exercise, euphemistically referred to as a 'Round Robin' analysis. Each participant was provided with the design and as-built information about the SCV model and the CS and was asked to predict the response (strains, displacements) of the model at 43 measurement locations as well as predicting the most likely failure mode and pressure. These results were compiled and published prior to the test (Luk et al., 1996) and a number of the participants met to discuss the results in October 1996. In general, there was fair agreement between the independent calculations, however, there was some disagreement in the interpretation of the analysis results relative to predicting failure.

These pretest analyses will be discussed in more detail in conjunction with the description of the test results.

HIGH PRESSURE TEST

The high pressure test of the SCV model was conducted on December 11-12, 1996, at Sandia National Laboratories. The conduct of the test is described (Luk et al., 1997, Luk et al.,

1998). Briefly, after approximately sixteen and a half hours of continuous, monotonic pressurization using nitrogen gas, the test was terminated when a tear developed at a pressure of 4.66 MPa (676 psig) or roughly six times the design pressure. Rapid venting of the model was observed and the pressurization system, operating at capacity (1300 scfm), was unable to maintain pressure in the model.

Posttest visual inspection of the interior of the model revealed a large tear, approximately 190 mm long, adjacent to the weld at the edge of the equipment hatch reinforcement plate (Fig. 2). The tear appears to have initiated at a point roughly 30 mm below the material change interface (around 8 o'clock when viewed from the inside) in the higher strength SPV490 shell, and propagated in both directions along the weld seam before it stopped. Interestingly, while the right hand side of the equipment hatch did not tear, significant necking was observed at a location symmetric with the tear.

In addition, a small meridional tear, approximately 85 mm long, was found in a vertical weld (at AZ. 201°) underneath a semi-circular hole in the hoop stiffener above the equipment hatch (Fig. 3). It appears that this small tear may have occurred first but did not grow and the pressurization system was able to compensate for any leakage through this tear. This tear also had a counterpart at a similar, diametrically opposed detail. While no tear developed at this location, necking in the weld was observed.

After this initial inspection of the interior of the model, the contact structure was removed to allow inspection of the exterior of the model. In addition to the observations noted above, visual inspection revealed evidence of the pattern of contact between the model and the CS in the form of crushed instrumentation lead wires and transfer of mill markings from the interior of the CS. Also, concentrated crack patterns in the paint indicated that global strains in the higher strength SPV490 shell were concentrated at the vertical weld seams (Fig. 4).

TEST RESULTS AND COMPARISON WITH PRETEST PREDICTIONS

More than 97% of the instruments survived the high pressure test. The gages which failed consisted primarily of those on the exterior of the model which were damaged when the model made contact with the CS. The raw strain data was corrected to compensate for temperature variations and cross-axis strains and the displacement data was corrected to account for any movement of the center reference column to which the displacement transducers were anchored. The complete data record is included in the SCV Test Report (Luk et al., 1998). A brief summary of the test data follows.

Local Response Adjacent to the Equipment Hatch

An extensive array of single element, strip and rosette strain gages were installed around the equipment hatch to get a relatively accurate map of the strain pattern. Figure 5 shows the locations of a few critical strain gages around the equipment hatch viewed from the inside of the model. A strip gage (STG-I-EQH-16) installed adjacent to the upper end of the large tear registered a maximum strain of 4.2 % and the two rosette gages (RSG-I-EQH-12 and -8) above it had recorded maximum strains of 3.7 % and 2.8 %, respectively. The rosette gage (RSG-I-EQH-22) slightly below the lower end of the tear recorded a maximum strain of 1.3 %. However, the highest strain reading of 8.7 % was recorded by a strip gage (STG-I-EQH-37) at 3 o'clock, just above the material change interface. Figure 6 shows the strain data recorded by these gages around the equipment hatch.

While the pretest calculations predicted failure in the vicinity of the equipment hatch at pressure levels very close to the actual failure pressure, a detailed comparison of the calculated and measured strains highlights some areas of discrepancy. First, visual observations indicate that the highest strains occurred in the higher strength SPV490 shell, below the material change interface, rather than in the weaker SGV480 shell as predicted by the analyses. Second, the near-field strains around the equipment hatch were almost double those predicted by the analysis. Finally, the locally thinned area which was the focus of concern in the pretest analysis, appeared to have little effect on the response in the vicinity of the equipment hatch.

Global Response

The global response of the SCV model was monitored using free-field strain gages and an array of internal displacement transducers which measured the strains and displacements at several elevations along 4 cardinal azimuths (0°, 90°, 180°, and 270°).

Maximum free-field hoop strains ranging from 1.7 to 2.0 % were measured at 4.5 MPa (560 psig) at the upper conical shell section (Fig. 7). Hoop strains calculated from the displacement measurements ($\Delta r/r$) were consistent with the strain gage measurements at these locations. The narrow range of strain variations suggests that the SCV model, excluding the area around the equipment hatch, behaved in a axisymmetric manner as expected.

Figure 8 shows the spatial variation of displacements at the cardinal azimuths at 4.5 MPa. It should be noted that the displacement pattern is fairly axisymmetric with the exception of 90°, the azimuth where the equipment hatch is located, where the displacements in the lower conical shell section, below the material change interface, are much larger than at the free-field azimuths (0°, 180°, and 270°). This is of particular interest in light of the fact that this area was actually 'pulled-in' during

fabrication of the SCV model and this is the area where the large tear occurred.

Figure 9 shows the spatial variation of displacement as a function of pressure at a representative free-field azimuth (270°). From this figure it appears that global yielding of the vessel occurred somewhere between 3 and 4 MPa, however, the pressure intervals chosen for this plot are not small enough to identify the yield pressure.

Figures 10 and 11 show the displacements at the middle and upper conical shell sections as a function of pressure and along with Fig. 7, indicate that the onset of global yielding may have occurred as early as 2.5 MPa and perhaps earlier at some azimuths. We can also infer from these figures that generalized contact between the SCV model and the CS began at approximately 4.0 to 4.5 MPa.

Figures 7, 10, and 11 also compare the pretest analysis predictions for global strains and displacements with the test results. The most significant observation from this comparison is that the pretest calculations significantly overpredicted the pressure at which global yielding occurred and continued to underpredict deformations and strains after yielding up to failure. This result is troubling since uniaxial tensile test data for the actual materials used in the fabrication of the model were used to define the material properties for analytical model and past experience had led us to expect good agreement between global response calculations and test results.

In attempting to understand the source of this disagreement, a comparison between the analytical results of several Round Robin participants and the test data was made (Fig. 12). This figure illustrates the effect of using the lower bound, average and actual results of uniaxial tensile test data to define the material properties of the model. From this comparison, it appears that the use of the lower bound data gave the best agreement with the test results. There may be a variety of factors which could contribute to the discrepancy between the analytical and test results (e.g., the effect of residual stresses), however, this comparison highlights the sensitivity of the analytical results to relatively small variations in the material models.

One other observation from this comparison is that it appears that the effective gap was larger than the nominal gap of 18 mm used in the pretest analysis. No attempt was made to characterize the as-built gap in the pretest analysis, even though this dimension varied from 13 to 24 mm after installation of the contact structure was complete.

Acoustic Emission Data

In addition to the strain and displacement transducers, twenty-four acoustic emission sensors (eighteen interior and six exterior) were installed on the model. Analysis of the data

collected by these sensors indicated two regions with high acoustic emissions during the test. One region located just below the equipment hatch began generating significant acoustic activity at approximately 4.25 MPa. The close proximity of this region to the equipment hatch suggests that significant material distress, leading to the large tear might have begun at this pressure. Another region had a significant increase in acoustic emissions beginning at 3.75 MPa, however, this region is not very close to the small tear, therefore it is not clear whether the initiation of the small tear is related to this pressure.

POSTTEST INSPECTION AND EVALUATION

In addition to the posttest visual inspection described above, a detailed metallographic evaluation of the SCV model was conducted to characterize the local failure mechanisms and, hopefully, provide some insight into both the global and local response of the vessel. This detailed evaluation and analysis is described (Van Den Avyle et al., 1998).

Briefly, sections were removed from the model surrounding the tears and areas of necking or other obvious structural distress. Fractographic inspection of the failure surfaces indicated that the tearing mechanism was ductile and did not display any evidence of flaws or other defects which might have acted to initiate failure. It was therefore concluded that failure occurred as a result of strains exceeding the limits of the material and it should be possible to characterize failure based on the material properties of the steel.

After this inspection, smaller sections were removed from the model and polished cross-sections normal to the surface of the model were examined using a scanning electron microscope to characterize the grain structure. Hardness tests were also performed on these polished specimens to look for variations in material properties. A section through the major tear surrounding the equipment hatch is shown in Fig. 13.

The results of these inspections revealed changes in the grain structure of the SPV490 material in the heat affected zone (HAZ) surrounding the reinforcement plate weld and a significant reduction in the hardness of the HAZ and adjacent parent material. Using well established relationships between hardness and tensile strength, these results indicate a significant reduction in tensile strength along with a corresponding, though less well defined, reduction in the yield strength of the material. These results indicate that one possible explanation for the strain patterns observed around the equipment hatch and in the weld seams of the SPV490 shell may be due to this localized microstructural alteration and reduced hardness and strength in the HAZ of the SPV490 alloy plate.

POSTTEST ANALYSIS PLANS

Considering the SCV test data, visual and metallographic posttest evaluations of the SCV model, and the pretest analysis

results, a posttest analysis plan has been developed to address the observed behavior of the model and address the inconsistencies between the pretest analysis results and the test data. The results of this posttest analysis will be published at a later date.

CONCLUSION

The high pressure test of the SCV model conducted at Sandia National Laboratories on December 11-12, 1996, was considered a success with regard to the specified test objectives:

1. The test provided experimental data for checking the capabilities of analytical methods well into the inelastic range of the model. While it appears that some generalized contact was occurring at the time of the failure, it is not clear that the data is adequate to confirm the validity of contact algorithms in the analysis codes.
2. The test confirmed the critical nature of discontinuities, such as penetrations, as potential failure mechanisms. While the pretest analyses did not predict the exact location of the tears, the strain-based failure criteria appeared to be consistent with the test results and resulted in good agreement with the actual failure pressure. The test also identified the potential significance of local changes in material properties due to welding and local fabrication details on potential failure modes. The measured global strains at failure of 2% are also consistent with previous tests of steel containment vessel models (Horschel et al., 1993).
3. The test and analytical results should provide useful information for the evaluation of prototypical containments and focus attention on critical details and analysis methodologies.

REFERENCES

Horschel, D. S., Ludwigsen, J. S., Parks, M. B., Lambert, L. D., Dameron, R. A., and Rashid, Y. R., June 1993, "Insights Into The Behavior of Nuclear Power Plant Containments During Severe Accidents," SAND90-0119, NPPRW-CON90-1, Sandia National Laboratories, Albuquerque, NM.

Luk, V. K., and Klamerus, E. W., 1996, "Round Robin Pretest Analyses of a Steel Containment Vessel Model and Contact Structure Assembly Subject to Static Internal Pressurization," NUREG/CR-6517, SAND96-2899, Sandia National Laboratories, Albuquerque, NM.

Luk, V. K., et al., August 18-22, 1997, "Testing of a Steel Containment Vessel Model", Proceedings of the 14th International Conference on Structural Mechanics in Reactor Technology, Lyon, France.

Luk, V. K., and Hessheimer, M. F., 1998 (to be published), "Design, Instrumentation and Testing of a Steel Containment Vessel Model," Sandia National Laboratories, Albuquerque, NM.

Porter, V. L., Carter, P. A., and Key, S. W., 1996,
"Pretest Analyses of the Steel Containment Vessel Model,"
NUREG/CR-6516, SAND96-2877, Sandia National Laboratories,
Albuquerque, NM.

Van Den Avyle, J. A., and Eckelmeyer, K. H., 1998,
"Posttest Metallurgical Evaluation Results for the SCV High
Pressure Test," Sandia National Laboratories, Albuquerque, NM.

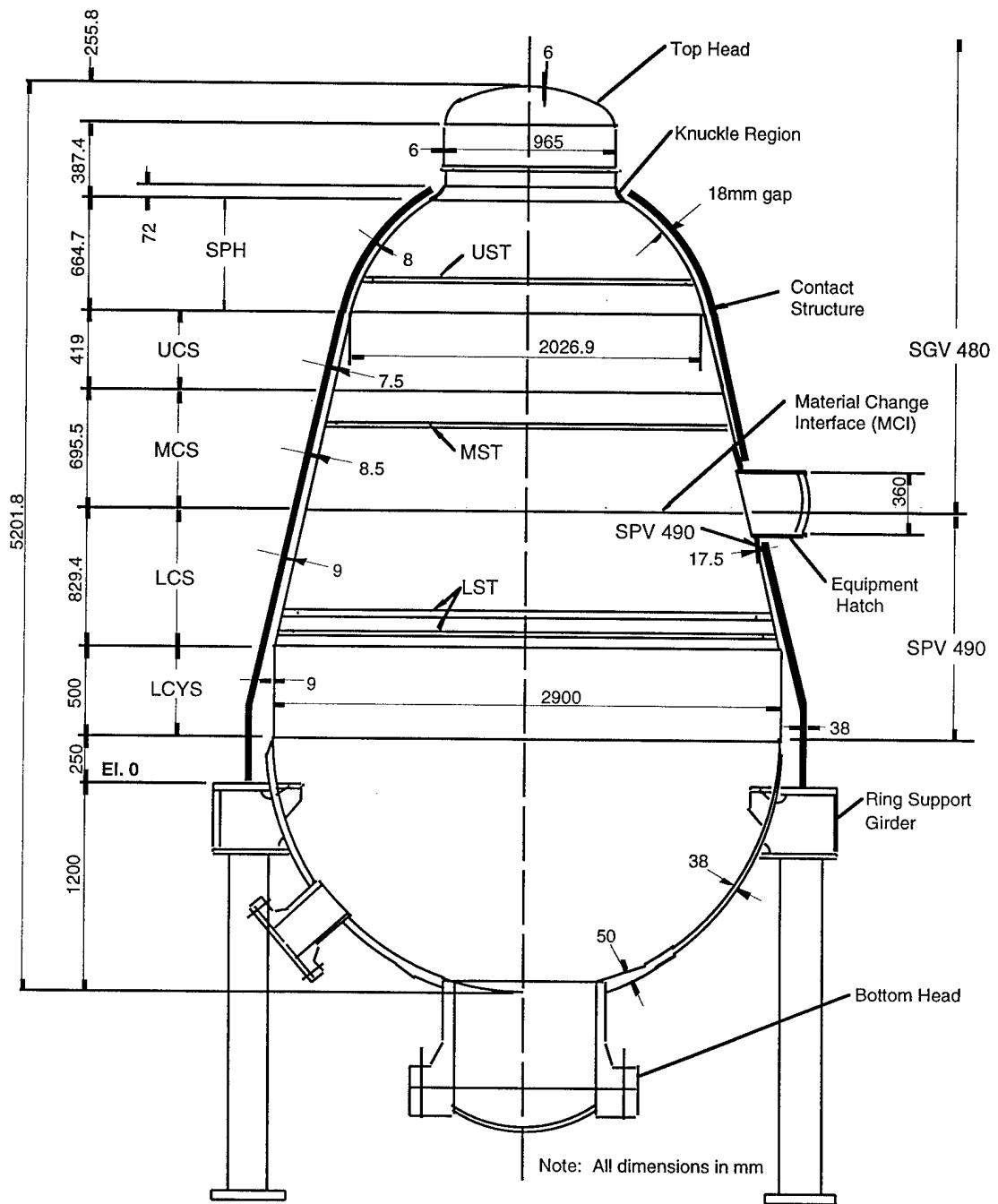


Figure 1. Elevation View of the SCV/CS Assembly

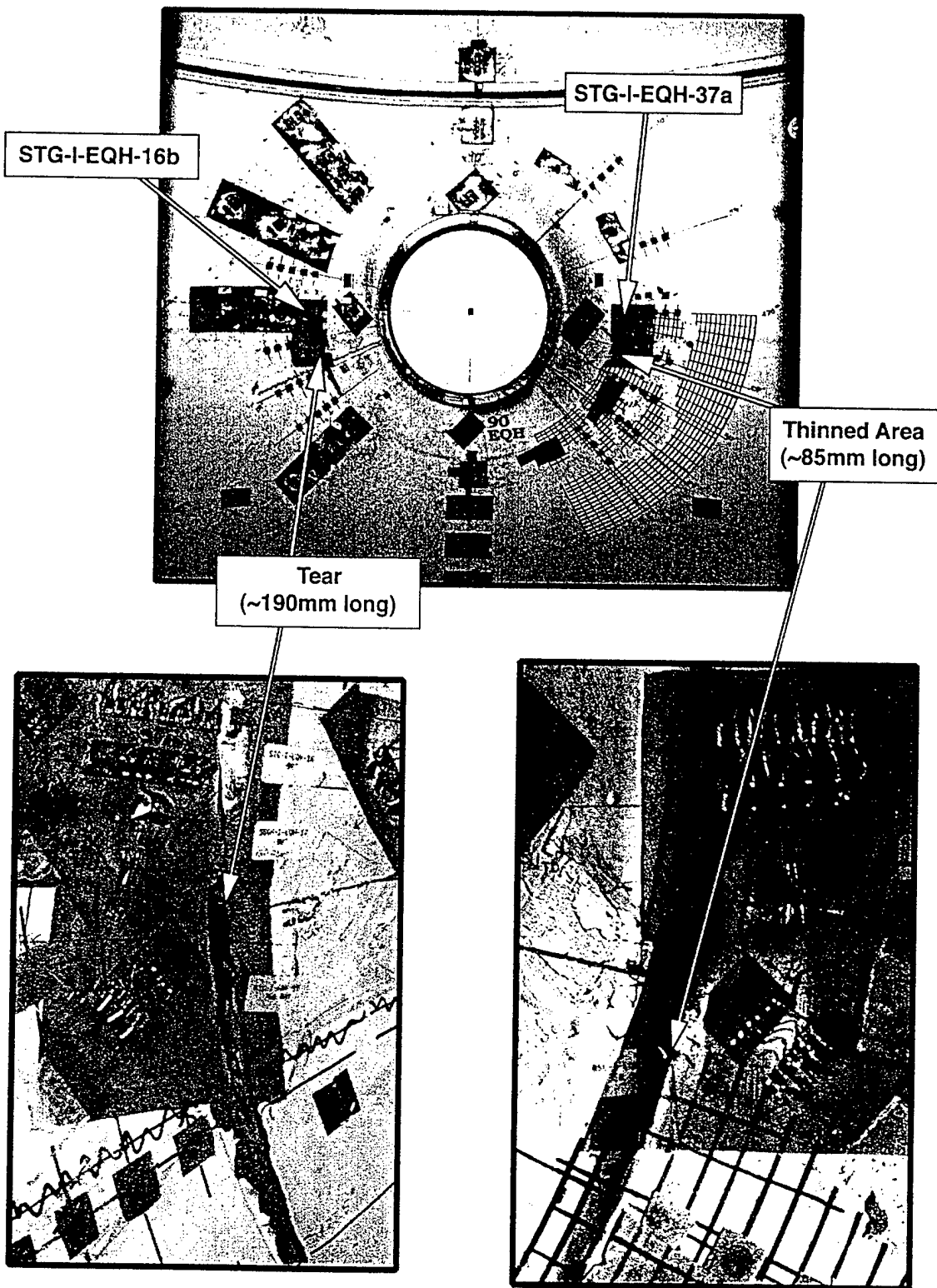
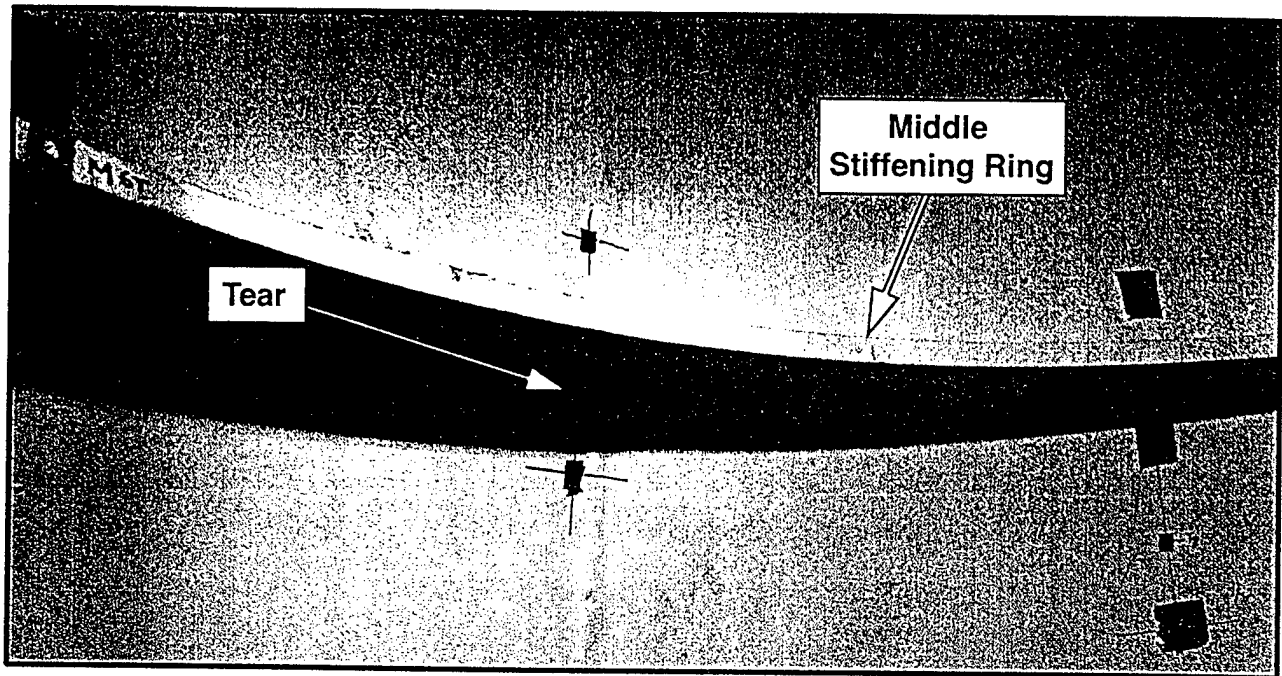
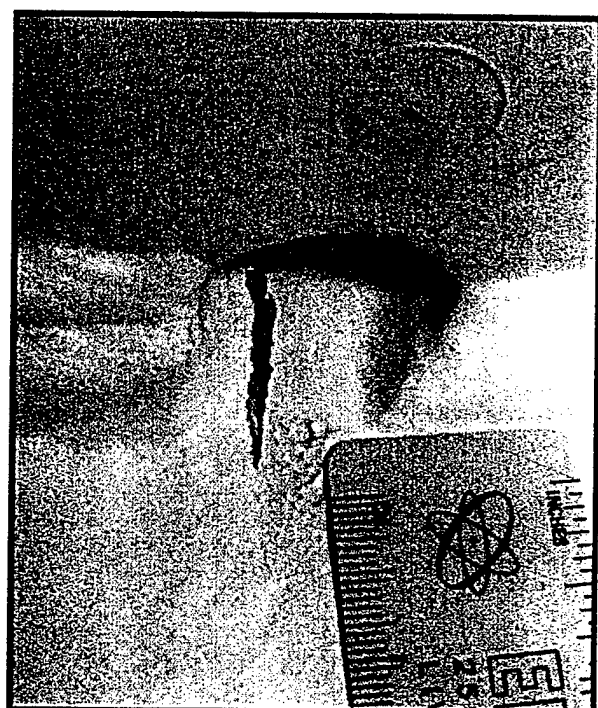


Figure 2. Interior Posttest View of the Equipment Hatch



Above



Below

Figure 3. Posttest View of Tear at Middle Hoop Stiffener Detail

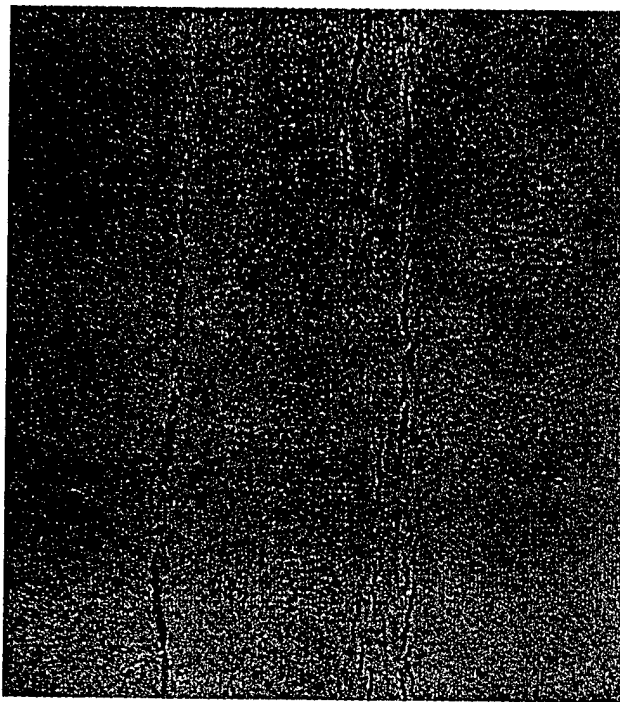


Figure 4. Posttest View of Vertical Weld Seam in Lower Conical Section (SPV490)

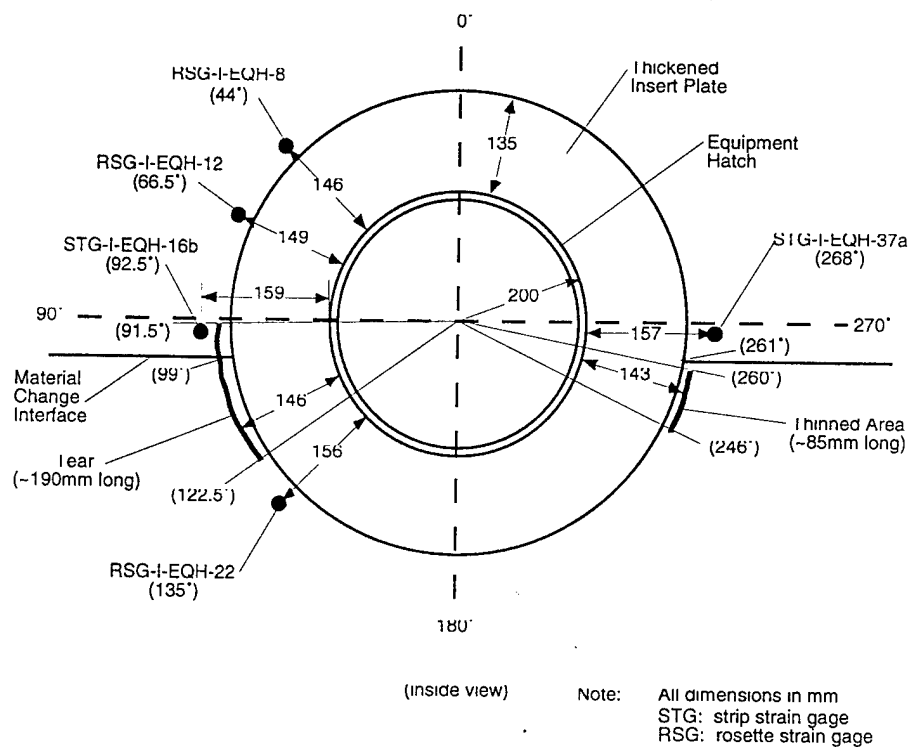


Figure 5. Interior Elevation of the Equipment Hatch

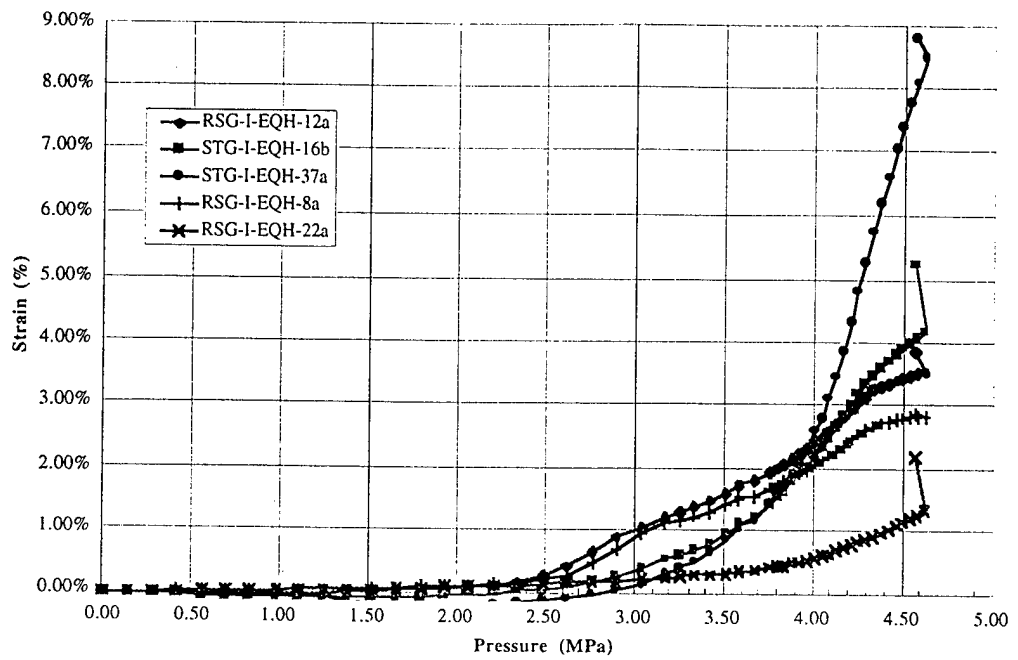


Figure 6. Strains Around Equipment Hatch

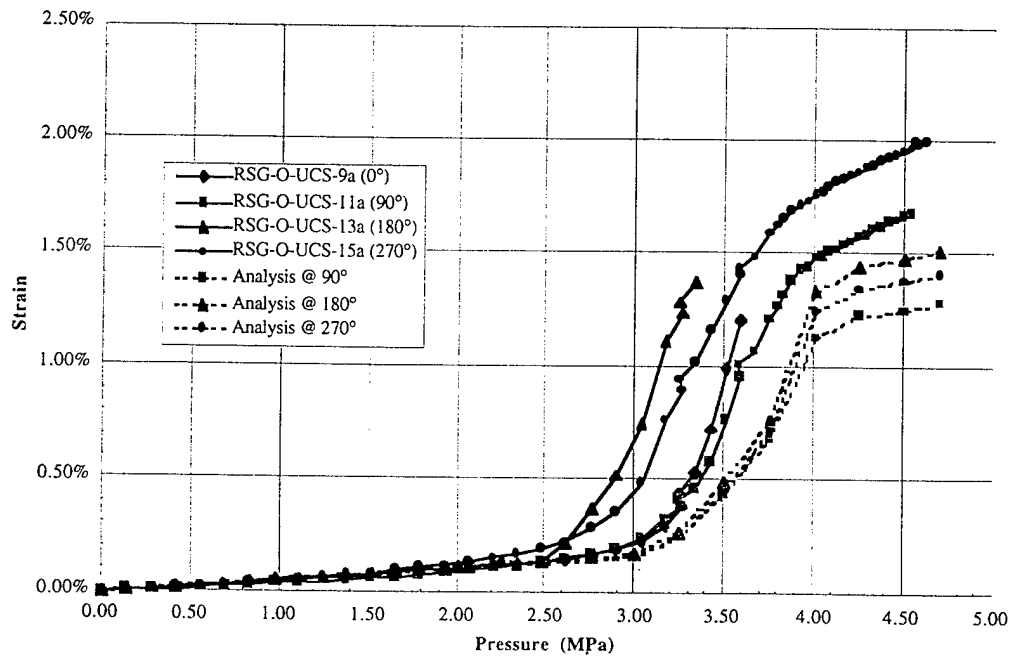


Figure 7. Hoop Strains @ Upper Conical Shell Section (UCS), EI. 2536 mm

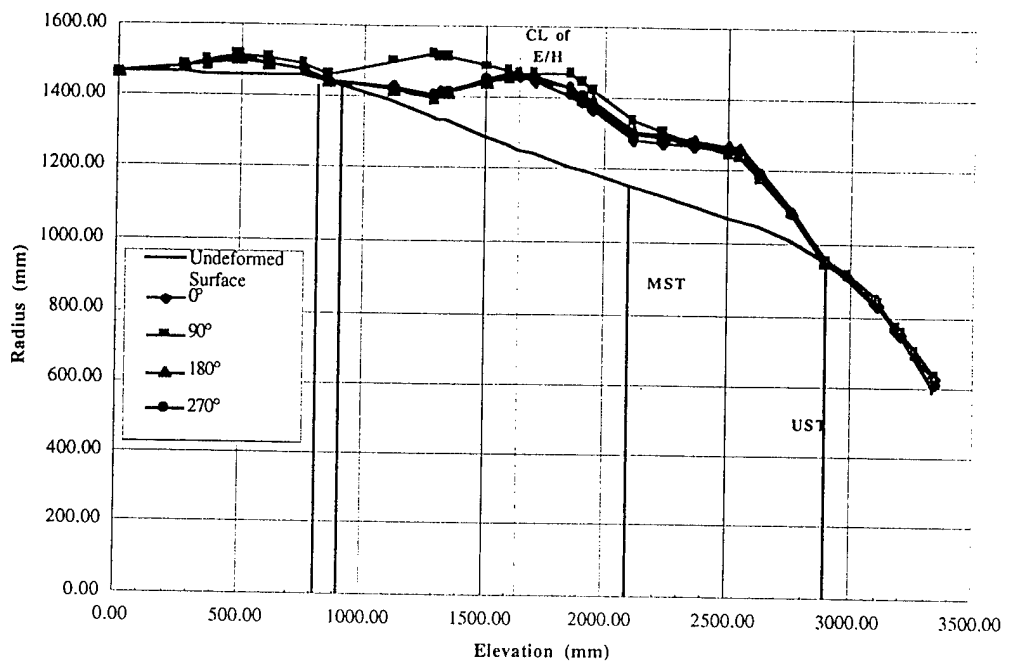


Figure 8. Displacement Contours (x10) @ 4.5 MPa

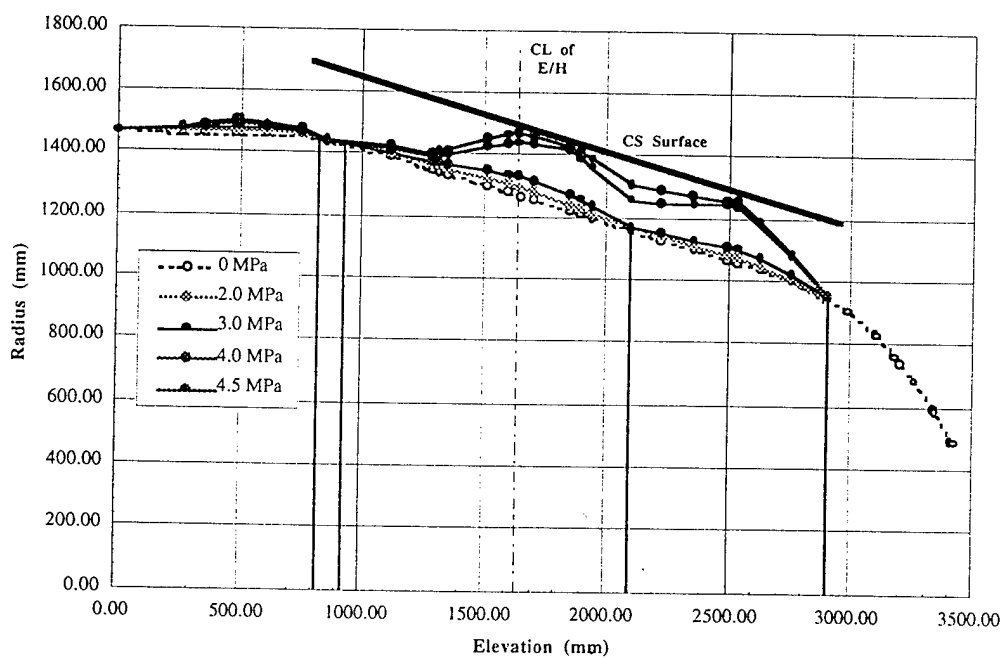


Figure 9. Displacement Contours (x10) @ 270°

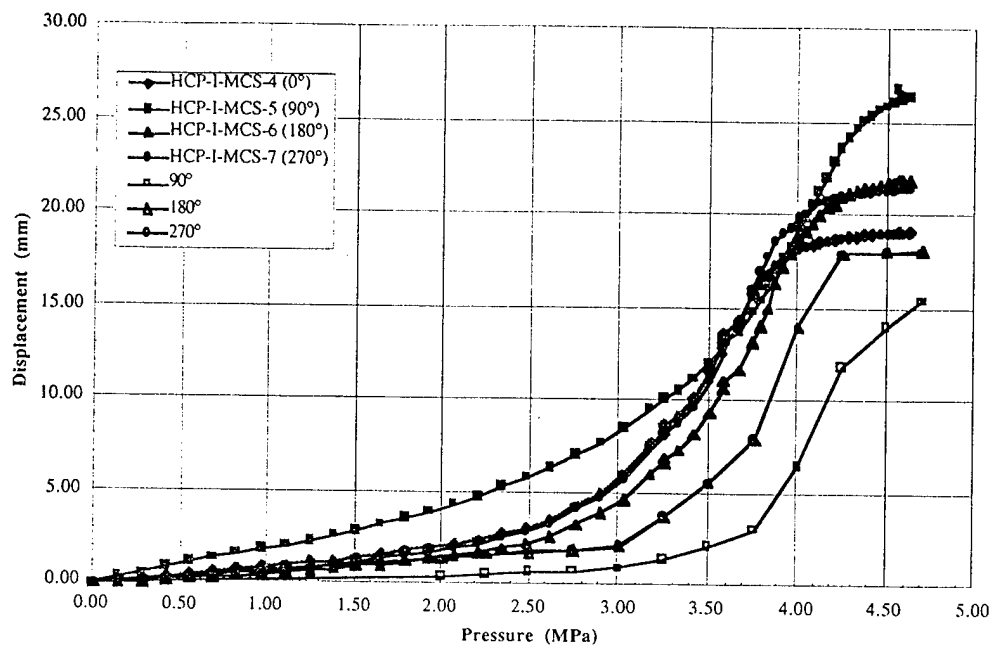


Figure 10. Radial Displacements @ Middle Conical Shell Section (MCS), El. 1850 mm

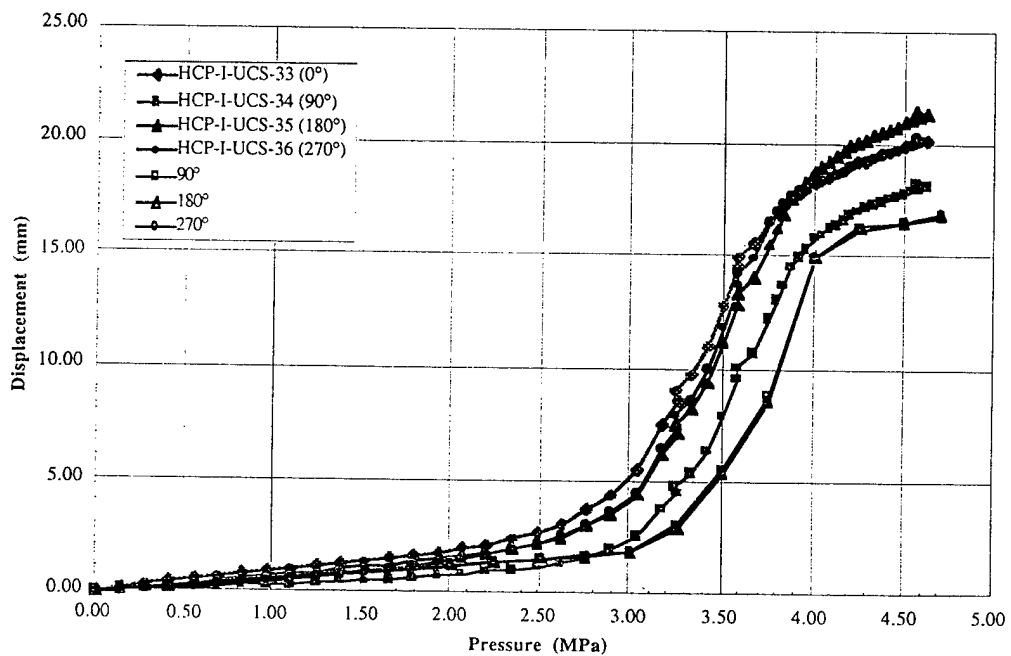


Figure 11. Radial Displacements @ Upper Conical Shell Section (UCS), El. 2536 mm

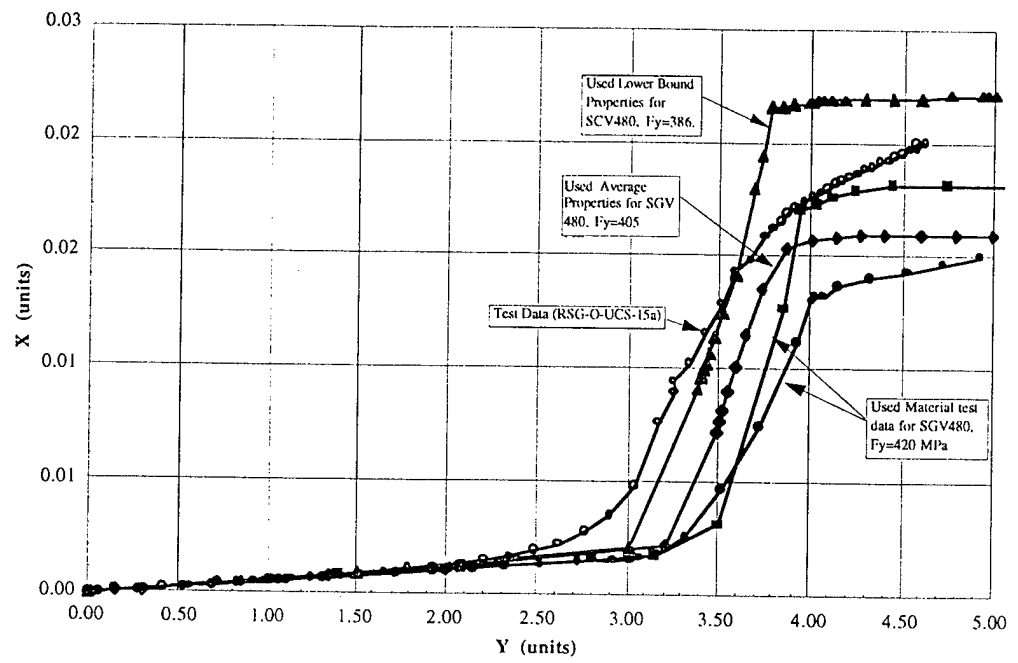


Figure 12. Hoop Strain @ Upper Conical Shell Section (UCS), El. 2536 mm

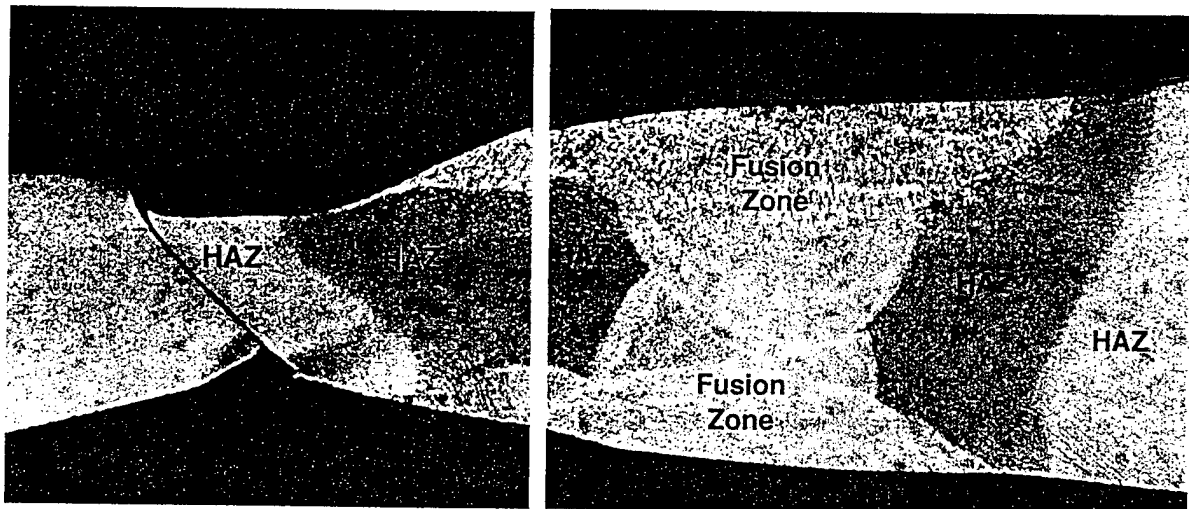


Figure 13. Cross-section through Large Tear @ Equipment Hatch

M98005459



Report Number (14) SAND -- 98-1044C
CONF-980708--

Publ. Date (11) 199805

Sponsor Code (18) NRC, XF

UC Category (19) UC-000, DOE/ER

19980706 052

DOE